AJNR

Epidural Fibrosis and Recurrent Disk Herniation in the Lumbar Spine: MR Imaging Assessment

Carl V. Bundschuh, Michael T. Modic, Jeffrey S. Ross, Thomas J. Masaryk and Henry Bohlman

AJNR Am J Neuroradiol 1988, 9 (1) 169-178
http://www.ajnr.org/content/9/1/169

Epidural Fibrosis and Recurrent Disk Herniation in the Lumbar Spine: MR Imaging Assessment

Carl V. Bundschuh[1, 2]
Michael T. Modic[1]
Jeffrey S. Ross[1]
Thomas J. Masaryk[1]
Henry Bohlman[3]

Twenty patients were enrolled in a prospective study to evaluate MR imaging in the differentiation of epidural scar and herniated disk material. Fourteen patients had surgical verification of imaging findings. In 12 (86%) of these patients, the MR interpretations fully agreed with the observations at surgery. Careful integration of the findings on sagittal and axial T1-weighted images with more T2-weighted axial images was important for analysis. Anterior and lateral recess scars were hypo- or isointense on T1-weighted sequences and hyperintense on more T2-weighted sequences relative to the "parent" anulus intensity. Free fragments demonstrated a slightly hyperintense signal intensity on T1-weighted images relative to epidural fibrosis but had a similar hyperintense signal intensity on T2-weighted sequences. Prolapsed or extruded disk fragments were hypo- or isointense relative to the parent anulus on all sequences.

Morphology, epidural location, mass effect, and often signal intensity were the important parameters by which scar and herniated disk could be differentiated with MR.

Epidural fibrosis and recurrent or residual disk herniation are among the common causes of the failed back surgery syndrome (FBSS) [1]. This syndrome is characterized by intractable pain and various degrees of functional incapacitation after removal of herniated lumbar intervertebral disk and/or bone. Its reported incidence ranges from 10 to 40% [1, 2].

Reoperation on scar tissue generally leads to a poor surgical result, in contradistinction to removal of herniated disk [3, 4]. The imaging goal, therefore, is to preoperatively distinguish scar from disk. When unenhanced CT is used in the preoperative assessment, scar can be separated from herniated nucleus pulposus (HNP) in approximately 43% of cases [5]. IV contrast-enhanced CT increases the rate of overall correct diagnosis from 74 to 87% [5–7]. Anecdotal reports by us and others suggest that MR may also have a role in the workup of FBSS [8, 9]. In particular, scar was shown to have an increased signal, and HNP decreased on images with longer echo times (TEs) and repetition times (TRs) [9]. To help further define the role of MR in distinguishing scar from HNP we undertook this prospective study on a group of FBSS patients with a high likelihood of reoperation. The surgical findings were compared with the MR interpretations to gain some measure of objective accuracy. IV CT, if available, was also entered into the analysis.

Subjects and Methods

Twenty patients (14 men and six women 18–72 years old; average age, 46.3 years) were admitted to the study from July 1985 to April 1986. The patients were referred for enrollment if clinical history and/or physical examination revealed the presence of the FBSS and there was a strong likelihood that further surgery would be required. Although not part of the entry criteria, most referring physicians requested a plain-film metrizamide myelogram and subsequent CT metrizamide myelogram as part of the diagnostic evaluation.

Of the 20 patients enrolled, 14 had repeat surgery and a complete MR examination. In nine of the 14, IV CT was performed also.

This article appears in the January/February 1988 issue of *AJNR* and the April 1988 issue of *AJR*.

Received April 14, 1987; accepted after revision September 10, 1987

[1] Department of Radiology, University Hospitals of Cleveland, Case Western Reserve University, Cleveland, OH 44106.

[2] Present address: Department of Radiology, Sentara Norfolk General Hospital, 600 Gresham Dr., Norfolk, VA 23507. Address reprint requests to C. V. Bundschuh.

[3] Department of Orthopaedic Surgery, University Hospitals of Cleveland, Case Western Reserve University, Cleveland, OH 44106.

***AJNR* 9:169–178, January/February 1988**
0195–6108/88/0901–0169

IV CT was performed on a Siemens DRH scanner operating at 125 kVp with 4-mm slices and 2-mm overlaps. The plane of section was angled to the disk space in question with the aid of a lateral scout image (topogram). The precontrast scan, obtained at 620 mAs, was initiated at the caudal midvertebral body and carried through the postoperative disk space to the cephalad midbody level. With the patient motionless, a 100-ml bolus of Angiovist 292 was injected through a heparin lock attached to an 18- to 21-gauge needle that had been placed prior to scanning. The postcontrast scan was then begun, usually from midbody to midbody, while the remaining 200 ml of contrast material was injected slowly. In an effort to optimize contrast resolution on the postcontrast scan and to prevent excessive tube heating, an 830 mAs technique was only used for the postcontrast set of images. Contrast differences were first optimized on the postcontrast scan (window ≈500, center ≈25) and then applied to precontrast images. Total examination time ranged from 45 to 60 min.

The MR examinations were performed on a 1.5-T superconductive unit* with a copper foil-wrapped, 12.7-cm-circular surface coil operating in a receive mode only. A 50-cm body coil served as the radiofrequency transmitter. A complete MR study consisted of four separate acquisitions. All sequences used a 256 × 256 acquisition and display matrix, 4-mm slice thickness, and 2-mm interslice gap. Sagittal sequences were both T1-weighted (TR = 500 msec, TE = 17 msec) and T2-weighted (TR = 2000 msec, TE = 90 msec). Axial T1-weighted (TR = 500 msec, TE = 17 msec), spin-density-weighted, and T2-weighted (TR = 2000 msec, TE = 30 or 90 msec) acquisitions were obtained angled to the disk space in question.

Preoperative IV CT and MR examinations were evaluated independently. With IV CT, the presence or absence of aberrant soft tissue within the bony spinal canal or neural foramina at the operated level was determined. Once identified, its location within the epidural space, enhancement characteristics, and presence or absence of mass effect were noted.

Plain CT and IV CT criteria for differentiating scar from disk have been discussed [5, 6, 10–14]. Briefly, scar has been said to enhance uniformly. It generally conforms to the available epidural space, is most prominent above or below the disk space, can retract the dural tube, and usually has a preenhancement density of 50–75 H. Recurrent HNP, on the other hand, has mass effect, occurs at the disk space, and is often directly contiguous with the anulus. Theoretically, it should not enhance. The density of disk material on the Siemens DRH scanner (field of view = 15 cm) is generally between 90 and 120 H, with free disk fragments occasionally appearing somewhat less dense.

Protruded or extruded disk herniations were prospectively predicted on MR if the abnormal soft-tissue mass was contiguous with the intervertebral disk (best seen on sagittal images), exhibited mass effect, was located in the anterior epidural space or lateral recess space, and was hypo- or isointense when compared with the parent anulus in all sequences. Free fragments, however, were found to be hyperintense on more T2-weighted images and also had mass effect.

Epidural scar was prospectively predicted when aberrant soft tissue lacked mass effect, was not directly contiguous with the intervertebral disk, was hyperintense on T2-weighted images when compared with the parent anulus [9], and was often associated with previous bone removal. Other items evaluated on the MR study where applicable were (1) appearance of the anterior internal vertebral veins and retrocorporeal anastomoses; (2) bone changes secondary to surgery, including lateral or posterolateral fusion; (3) artifacts; (4) facet subluxation; (5) lateral and/or central stenosis; and (6) abnormal paraspinal muscle intensity.

* Siemens Magnetom.

Before surgery, all imaging studies were reviewed with the surgeon and predictions were made by the radiologist as to the nature of the observed abnormal extradural soft tissue. The surgeon subsequently and methodically identified all aberrant soft tissue seen on the presurgical imaging studies and noted its composition by location (for example, scar in the left epidural space, free disk fragment in the lateral recess).

Results

Table 1 summarizes the MR, surgical, and IV CT findings.

At surgery one patient had a herniated disk only, nine had both scar and bulging or herniated disk, three had scar only, and one had both scar and bony foraminal stenosis. In 12 of the 14 patients all MR findings were confirmed at surgery. Of the MR scans that were inconsistent with surgical findings (cases 4 and 8), one revealed what appeared to be a small disk anterior to a large scar occupying the right anterior and lateral epidural space (Fig. 1). This predicted herniated disk was not documented at surgery. In the other case, MR predicted a small scar, and a much larger one was actually found (Fig. 2).

The morphologic configuration of the protruded and extruded disk (Fig. 3) material in this study was consistent on both the axial and sagittal images and demonstrated contiguity of the aberrant soft tissue with remaining disk. Signal intensities were consistent with those reported previously and were either isointense with the anulus of the disk of origin or hypointense on all imaging sequences.

Free fragments were seen at or near the disk space, were well circumscribed, and exerted mass effect. When related to the disk of origin, two were increased on T1-weighted images and two were isointense. All four were hyperintense on both spin-density- and T2-weighted images (Figs. 2 and 4).

The anterior internal vertebral veins and retrocorporeal anastomoses were a potential cause of confusion and had a variety of axial MR appearances. Marked hypointensity was the most common finding on all imaging sequences (Fig. 5), although hyperintensity was noted occasionally on T1-weighted images and less often on the other sequences (Fig. 6).

The intensity characteristics of epidural scar varied according to location. All anterior scars were hypo- to isointense relative to the adjacent anulus on T1-weighted images, obliterating the high signal intensity of the normal epidural fat, and were hyperintense on spin-density- and T2-weighted sequences. In general, lateral scars exhibited similar characteristics, but not as consistently. More posteriorly toward the laminectomy site, the signal intensity of the scar became even more variable. However, increased signal intensity was generally seen in the paraspinal musculature at the operative site with T2-weighted acquisitions in the sagittal plane.

Of the nine patients in whom IV CT was performed, IV CT and surgical results agreed in eight. The surgical findings in this group included six herniated disks and surrounding scars, one epidural scar only, one scar and stenosis, and one anular bulge and scar (with the scar entrapping a nerve root). The one disagreement (IV CT in case 4) was rated as such because it was an indeterminate study (Fig. 2). A nonenhanc-

TABLE 1: Correlation of MR and IV CT with Surgical Findings in Failed Back Surgery Syndrome

Case No.	Surgery	MR Agreement	T1	T2	SD	IV CT Agreement
1	L ant extruded disk L5–S1	Yes	Hypo	Hypo	Hypo	Yes
	R ant epidural scar	Yes	Iso	Hyper	Hyper	Yes (enhancing)
2	L lat recess free disk fragment L4–L5	Yes	Iso	Hyper	Hyper	Yes
	L lat recess scar	Yes	Iso	Hyper	Hyper	Yes (enhancing)
3	L neuroforaminal prolapsed disk L5–S1	Yes	Iso	Iso	Iso	Yes
	Ant midline & L lat scar	Yes	Iso	Hyper	Hyper	Yes (enhancing)
4	L lat recess free fragment L4–L5	Yes	Iso	Hyper	Hyper	No (enhancing)
	Large L ant, L recess, & L lat scar	No: small ant scar No: small lat recess scar	Hypo Hypo	Hyper Hypo	Hyper Hypo	Yes (enhancing)
5	R, L ant, & R, L lat scar L4–L5	Yes	Iso	Hyper	Hyper	Not performed
6	Ant, L lat, & L lat recess scar & bony foraminal stenosis L3–L4	Yes	Iso	Hyper	Hyper	Enhancing ant and lat recess scar; nonenhancing lat scar (? streak or beam-hardening artifact)
7	L lat recess free disk fragment L5–S1	Yes	Hyper	Hyper	Hyper	Not performed
8	R ant & lat scar L5–S1	No: R ant disk Yes: ant & lat scar	Hypo Iso	Hyper Hyper	Hyper Hyper	Not performed
9	R lat recess scar L4–L5	Yes	Hyper	Iso	Hyper	Not performed
10	R ant & lat recess free fragment L5–S1	Yes	Hyper	Hyper	Hyper	Yes (enhancing)
	R ant & R lat scar	Yes	Iso	Hyper	Hyper	
11	L lat recess extruded disk L4–L5	Yes	Iso	Iso	Iso	Yes
	L ant scar	Yes	Iso	Hyper	Hyper	Yes (enhancing)
12	R ant extruded disk L5–S1	Yes	Iso	Iso	Iso	Yes
	R ant scar	Yes	Iso	Hyper	Hyper	Yes (enhancing)
13	Bulging disk L4–L5	Yes	Iso	Iso	Iso	
	R lat scar	Yes	Iso	Hyper	Hyper	Yes (enhancing)
14	L ant free fragment	Yes	Iso	Hyper	Hyper	Not performed
	L ant, L lat recess, & L lat scar	Ant & lat recess scar	Iso	Hyper	Hyper	

Note.—In prolapse, the herniated nucleus pulposus (HNP) is confined by outer anulus; in extrusion, HNP extends beyond anulus; with free (sequestered) fragment, HNP is no longer in contact with parent nucleus. T1 = T1-weighted sequence; T2 = T2-weighted sequence; SD = spin-density-weighted sequence; L = left; R = right; ant = anterior; lat = lateral; hypo = hypointense relative to anulus of "parent" intervertebral disk; hyper = hyperintense; iso = isointense.

ing hypodense left L5 lateral recess mass was thought to represent either a swollen L5 nerve root or a small free disk fragment. At a slightly more caudal portion of the lateral recess and the left anterior epidural space, there was a heterogeneously enhancing mass consistent with either scar or free disk. Surgery revealed a large free disk fragment in addition to a mildly swollen L5 nerve root in the above locations. Because the IV CT study at these levels was ranked indeterminate before surgery, it was rated a disagreement; however, at the mid-L4 level, scar was correctly predicted.

All of the surgically confirmed anterior epidural or lateral recess scars and five of six lateral epidural scars were believed to enhance with IV CT. Six of nine posterior scars enhanced. In the comparison of IV CT and MR, there was good agreement in the identification of herniated disk and lateral recess or anterior scar, where MR had demonstrated high signal on spin-density- and T2-weighted images. There was less agreement posteriorly, where fewer scars appeared to be of increased intensity on spin-density- or T2-weighted images than were seen to enhance on IV CT. In addition, IV CT appeared to better depict what had been reported to represent dural tube or perineural scarring in one patient [6]. No abnormal signal intensity could be appreciated on MR in these locations. IV CT demonstrated enhancement of the peripheral portion of several minimally bulging disks, a free disk fragment, and the exposed disk surface at a grade 2 spondylolisthesis. Increased signal intensity on the axial spin-density- or T2-weighted images was found only with the latter two IV CT findings.

In case 4, the MR findings of a herniated free disk fragment appeared more obvious than on IV CT findings because the substantial mass effect was better appreciated on MR. In addition, there was confusion on IV CT over whether the nonenhancing mass was a free disk fragment or an entrapped nerve root.

Certain miscellaneous findings are worthy of note. Post-

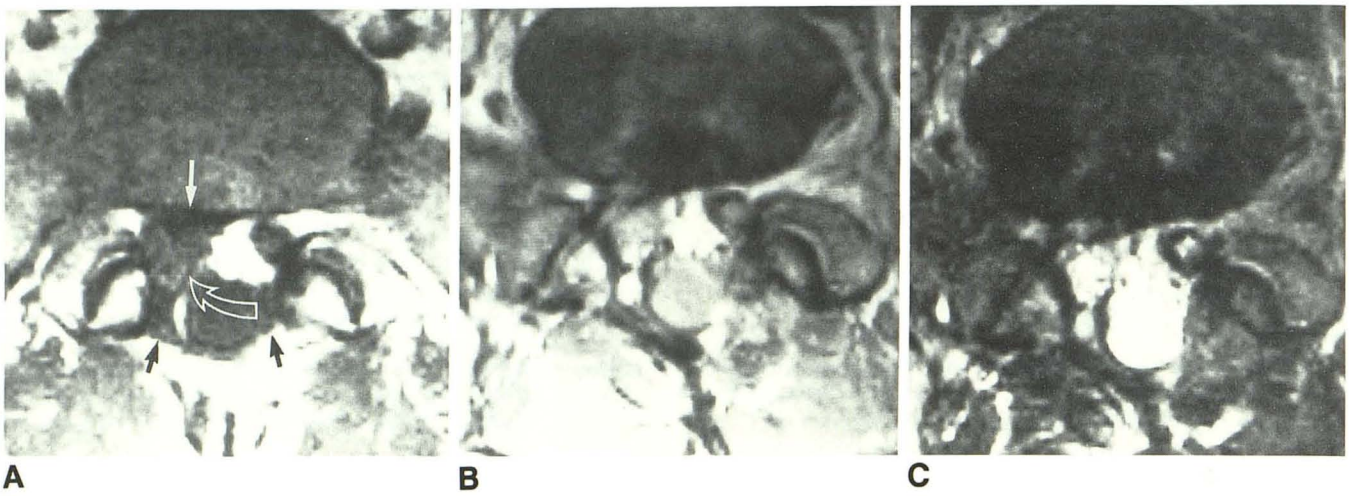

Fig. 1.—Case 8: epidural scar.

***A*, Axial image (TR = 500 msec, TE = 17 msec) at superior endplate of S1. Large abnormal soft-tissue structure (*curved arrow*), which is isointense with thecal sac and left S1 nerve root, is present, with more hypointense structure located anteriorly (*straight white arrow*). This soft-tissue structure appears to encompass region of right S1 nerve root. Laminectomy site (*black arrows*).**

***B* and *C*, Axial images at L5–S1 level. TR = 2000 msec, TE = 30 (*B*) and 90 (*C*) msec. Signal intensity of soft-tissue structure appears to parallel that of CSF within thecal sac, and to a lesser extent, epidural fat. Anterior structure that was hypointense on T1-weighted image is now slightly increased in signal intensity. This soft-tissue structure was predicted to represent herniated free disk fragment. At surgery, only exuberant epidural fibrosis was identified in same location as soft-tissue mass surrounding S1 nerve root. Epidural fibrosis was also noted in posterior laminectomy site on right, which also shows increased signal intensity on these more T2-weighted sequences (*A*, *black arrows*).**

operative bone changes were well appreciated on IV CT and, although not as conspicuous, were identified on axial MR images as focal areas of marrow disruption (laminectomy) or contour changes of the cortex of the apophyseal joints (facetectomy). Facet subluxation, spurious pseudomeningoceles, and conjoint nerve roots (Fig. 7) were readily identified with MR, and MR findings were similar to those of plain CT and IV CT. Lateral or posterolateral fusion masses often appeared centrally hyperintense on T2-weighted axial images, presumably because of their marrow content. A large signal void was noticed on one MR study without evidence of an abnormality on CT. However, a metal drill had been used during the interbody fusion procedure, and we presume that small metal filings were responsible for the MR artifact. Lateral bony stenosis was suggested when the lateral recess or neural foramen was narrowed by markedly hypointense structures representing cortical bone. All bone changes, whether degenerative or secondary to surgical intervention, were more obvious on IV CT, although with some experience similar findings could be identified on MR.

Discussion

FBSS has many causes. Excluding spondylolisthesis, the most significant lesions associated with this syndrome are recurrent/residual disk herniation, epidural fibrosis (scarring), lateral and/or central stenosis, and adhesive arachnoiditis [1, 14]. Other factors that are each believed to be responsible for less than 5% of cases are (1) direct nerve injury, (2) chronic mechanical pain, (3) pseudoarthrosis, and (4) wrong-level or wrong-side surgery [1]. It is important to distinguish scar from disk preoperatively, as removal of scar tissue generally leads to a poor surgical result when unaccompanied by disk material [3, 4]. In one study that followed 52 postoperative patients who underwent reoperation, only one patient with exclusive scar had long-term pain relief [4]. In all likelihood, this was from the propensity of epidural scar to become at least as exuberant as it was before removal.

Only brief accounts of the MR appearance of the postoperative spine exist in the radiology literature [9]. In general, the T2-weighted signal intensity of scar has been reported to be increased when compared with the adjacent postoperative intervertebral disk. Our study, although small, indicated that, by using the criteria of epidural location, morphologic configuration, signal intensity, and mass effect, MR has an accuracy comparable to IV CT for the identification of surgically remedial pathology.

Sagittal and axial images together were complementary in the evaluation. Axial sections provided an excellent depiction of the spatial distribution of aberrant soft tissue and reliable determination of the presence or absence of mass effect. The signal intensity of extrathecal soft tissue was better appreciated on axial than on sagittal images; however, the latter helped demonstrate contiguity of aberrant soft tissue when present with disk, thus suggesting herniation. Reviewing the signal intensity of the "mass" on axial T1-, spin-density-, and T2-weighted acquisitions together allowed an accurate prediction of the type of herniation and reliably distinguished protruded fragments from scar tissue (Fig. 3). This differentiation requires careful scrutiny because it can be difficult on MR to differentiate a free fragment from scar in the anterior epidural space or lateral recesses.

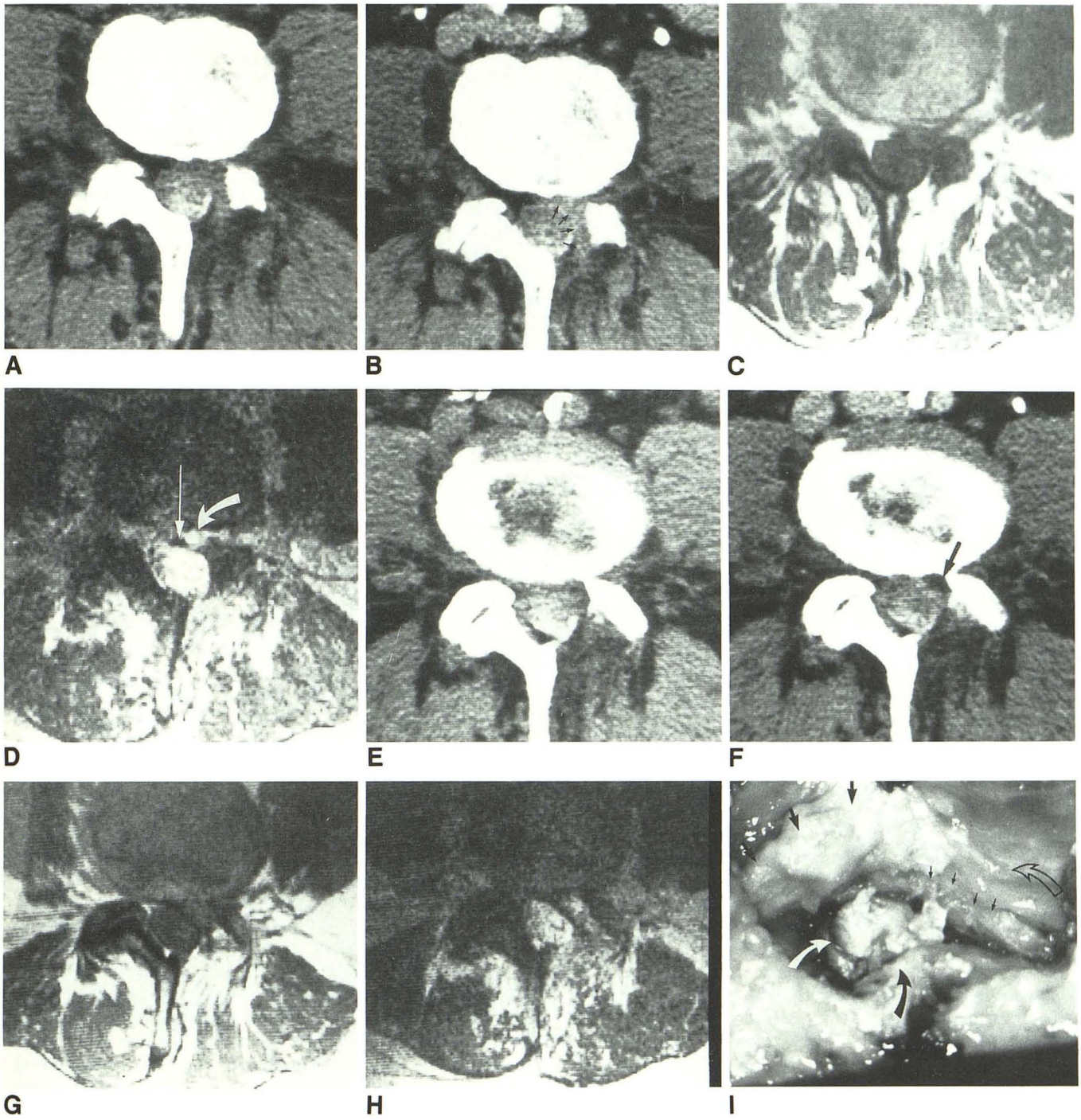

Fig. 2.—Case 4: free disk fragment and epidural scar.

***A* and *B*, Pre-(*A*) and post-(*B*) contrast IV CT scans at lower L4 level. Uniform enhancement of curvilinear scar occupying left anterior, lateral, and posterior epidural space as well as lateral recess (*arrows*). Note residual water-soluble contrast material remaining in thecal sac 1 day after CT metrizamide myelogram.**

***C*, Axial MR image (TR = 500 msec, TE = 17 msec) at lower L4 level. All components of epidural scar are hypointense.**

***D*, Axial MR image (TR = 2000 msec, TE = 90 msec) at lower L4 level. Only left anterior scar is bright (*curved arrow*). Ventral midline hypointensities (*straight arrow*) represent portion of anterior internal venous system.**

***E* and *F*, Pre-(*E*) and post-(*F*) contrast IV CT scans at inferior end plate of L4 (2 mm caudal to *A* and *B*). Hypodense, nonenhancing left L5 lateral recess mass is consistent with free disk fragment or swollen nerve root (*arrow*).**

***G*, Axial MR image (TR = 2000 msec, TE = 30 msec) at L4–L5 disk level shows isointense left lateral recess structure with mass effect.**

***H*, Axial MR image (TR = 2000 msec, TE = 90 msec) at L4–L5. Lateral recess mass is now hyperintense, suggesting scar, but because of mass effect abnormal soft tissue is more consistent with free fragment. High signal intensity is also seen in tissues at laminectomy site and in paraspinal musculature.**

***I*, Intraoperative photograph. Top of photograph is posterior aspect of patient, left is superior. Naked left superior articular facet of L5 (*curved solid black arrow*) cradles free disk fragment (*white arrow*) in lateral recess. *Small straight black arrows* delineate traversing left L5 root sleeve; *larger straight black arrows* designate curvilinear epidural scar. *Open arrow* depicts unaffected dural tube at mid L5 level.**

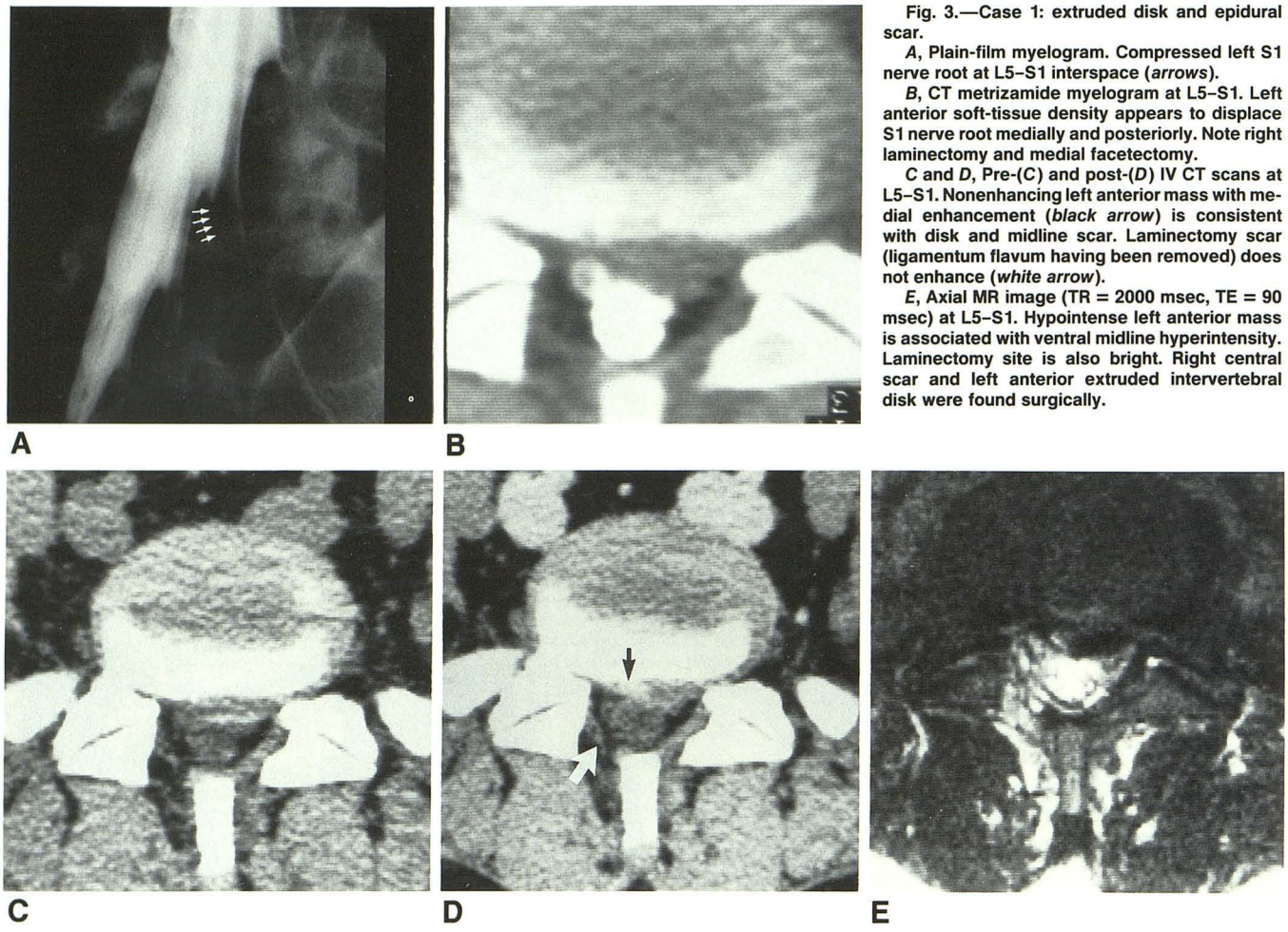

Fig. 3.—Case 1: extruded disk and epidural scar.

***A*, Plain-film myelogram. Compressed left S1 nerve root at L5–S1 interspace (*arrows*).**

***B*, CT metrizamide myelogram at L5–S1. Left anterior soft-tissue density appears to displace S1 nerve root medially and posteriorly. Note right laminectomy and medial facetectomy.**

***C* and *D*, Pre-(*C*) and post-(*D*) IV CT scans at L5–S1. Nonenhancing left anterior mass with medial enhancement (*black arrow*) is consistent with disk and midline scar. Laminectomy scar (ligamentum flavum having been removed) does not enhance (*white arrow*).**

***E*, Axial MR image (TR = 2000 msec, TE = 90 msec) at L5–S1. Hypointense left anterior mass is associated with ventral midline hyperintensity. Laminectomy site is also bright. Right central scar and left anterior extruded intervertebral disk were found surgically.**

As noted in our study, the signal intensity of free disk fragments can be increased relative to the anulus, particularly on T2-weighted sequences. Similar signal-intensity changes can also be observed in epidural scar (Fig. 8). In our small group of patients, half the surgically proved free disk fragments also showed a hyperintensity on the T1-weighted sequences relative to epidural fibrosis or anulus. As shown in Table 1, no surgically demonstrated free disk fragment appeared hypointense relative to the anulus. Scar, on the other hand, appeared slightly hypointense or isointense on the T1-weighted image where it could be separated easily from fat, which is hyperintense. Without the subtle difference in signal intensity of the posteromedial scar and free disk on the T1-weighted image in case 10 (Fig. 4), we would have predicted that only free disk material occupied the right anterior epidural space and lateral recess. This distinction is much less obvious on the T2-weighted sequences. Also, both epidural scar and fat usually conform to the available space, while herniated disk tends to compress and distort it. Therefore, mass effect may be the only finding that will aid in the discrimination of free disk fragment and anterior or lateral recess scar.

Exceptions to these patterns may exist, however, that make the intensity differences cited above just guidelines, at best. The morphology of the aberrant soft tissue and the presence or absence of mass effect may be the best indicators of the presence or absence of HNP (Fig. 4).

The mechanism for hyperintensity of scars on T2-weighted images is not understood. It could be related to an increase in spin density relative to dense fibrosis or peripheral anulus [20]. Likewise, the reason for the increased signal intensity of free fragments, when compared with protruded or extruded herniated disk fragments, is unknown. It is possible that in these free fragments more nuclear material has been extruded relative to anular material. With a 4-mm slice thickness, there is less problem with partial-volume averaging, which may explain why earlier reports with a 10-mm slice thickness more consistently demonstrated decreased signal intensity of disk fragment [8, 9, 16].

The variable appearance of the lumbar vertebral veins could complicate the differential diagnosis of an anterior nodular structure. The common marked hypointensity, when noted on all axial sequences, could be explained by high-velocity signal loss [21] (Fig. 6). Conversely, hyperintense veins on all sequences could be attributed to slow laminar flow (that is, flow-related enhancement) (Fig. 7), and were best appreciated near the entry slice of a multisection acquisition [18]. Since

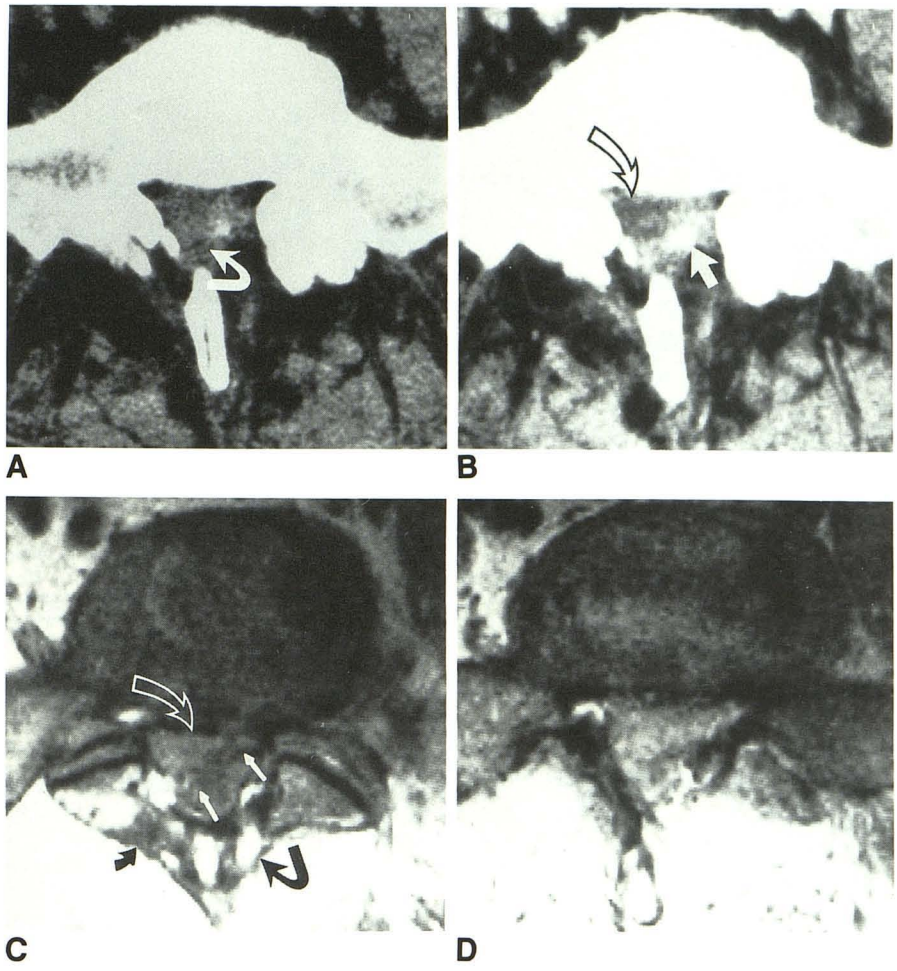

Fig. 4.—Case 10: free disk fragment and scar.
***A* and *B*, Pre-(*A*) and post-(*B*) IV CT scans at lateral superior endplate of S1. Nonenhancing right anterior and recess herniated disk fragment (*open arrow*) with enhancing posterior and medial scar (*straight white arrow*) are suggested. Thecal sac is largely obliterated (*solid curved arrow*). Mild enhancement is present at both laminectomy sites.**
***C*, Axial MR image (TR = 700 msec, TE = 17 msec) at superior endplate of S1. Hyperintense right anterior and lateral recess mass (*open arrow*) is covered by isointense left posteromedial band of soft tissue (*straight arrows*). Note isointense right and generally hyperintense left laminectomy sites (*short* and *long curved black arrows*, respectively).**
***D*, Axial MR image (TR = 2000 msec, TE = 30 msec) at superior endplate of S1. All aberrant soft tissue in ventral and right lateral canal is now hyperintense. At surgery, a free disk fragment with left posteromedial scar was found. Free disk fragment was predicted because of mass effect and hyperintense appearance of aberrant soft tissue on all imaging sequences. T1-weighted image helps separate hyperintense free fragment from isointense scar.**

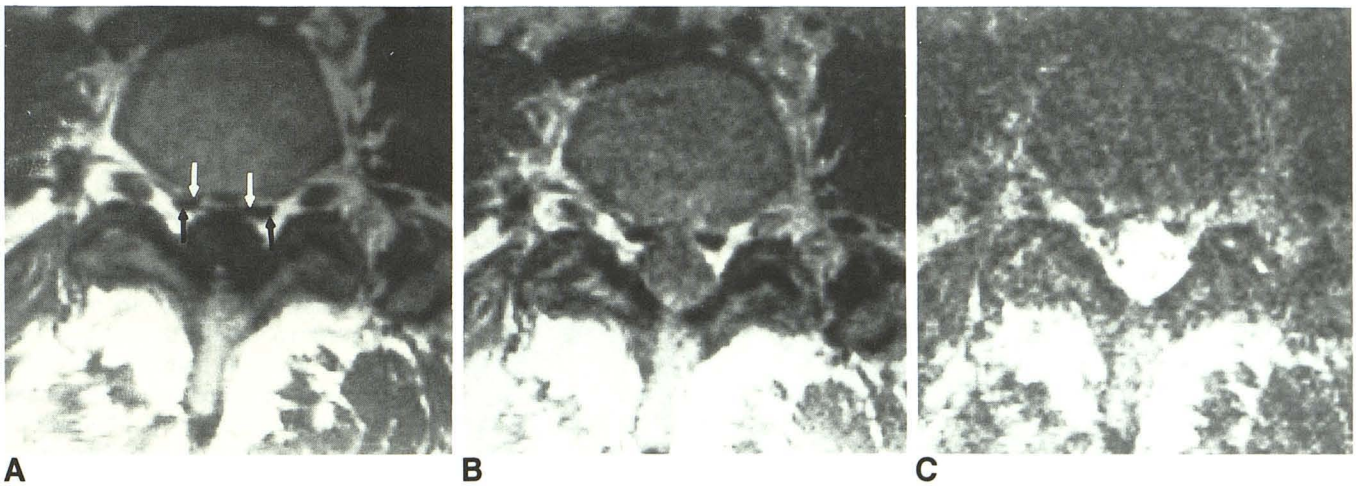

Fig. 5.—Normal patient. Axial MR images at lower L4 level. TR = 500 msec, TE = 17 msec (*A*); TR = 2000 msec, TE = 30 msec (*B*); TR = 2000 msec, TE = 90 msec (*C*). Hypointense appearance of medial (*white arrows*) and lateral (*black arrows*) right and left anterior internal vertebral veins is well appreciated on all sequences.

most venous blood flow is weakly cardiosynchronous as well as laminar [22], there is a potential for the occurrence of cardiac pseudogating. Ebb and flow in the vertebral veins has been established under physiologic conditions; a flow rate of approximately 5–7 cm/sec has been estimated to occur in veins of similar size [15]. Therefore, a laminar flow rate of 1–10 cm/sec, depending on physiologic conditions and the addition of an occasional pseudogating effect, could explain

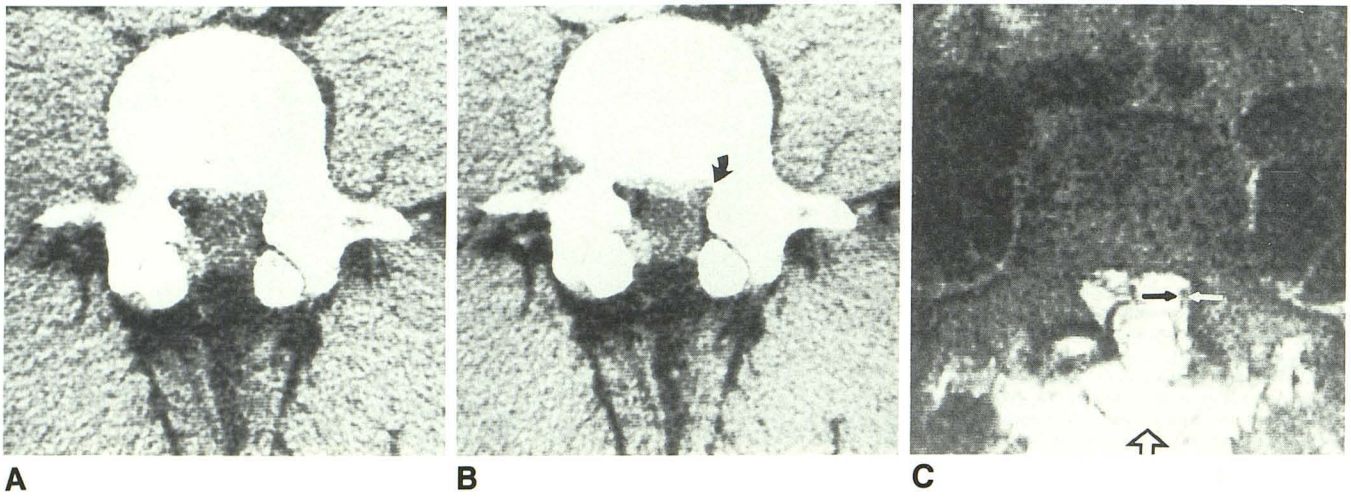

Fig. 6.—Case 6: epidural scar and bony foraminal stenosis.

A and *B*, Pre-(*A*) and post-(*B*) IV CT scans at mid L4 level. Enhancement of soft tissue in anterior epidural space and left lateral recess with small rounded structure of lower attenuation within (*arrow*).

C, Axial MR image (TR = 2000 msec, TE = 90 msec) at mid L4 level. Soft tissue in anterior epidural space is noted to be hyperintense and extends to left lateral epidural space. Hypointense left L4 nerve root is again noted (*solid arrows*), surrounded by high signal intensity of anterior and lateral epidural scar. Predominantly fatty tissue (*open arrow*) is at laminectomy site.

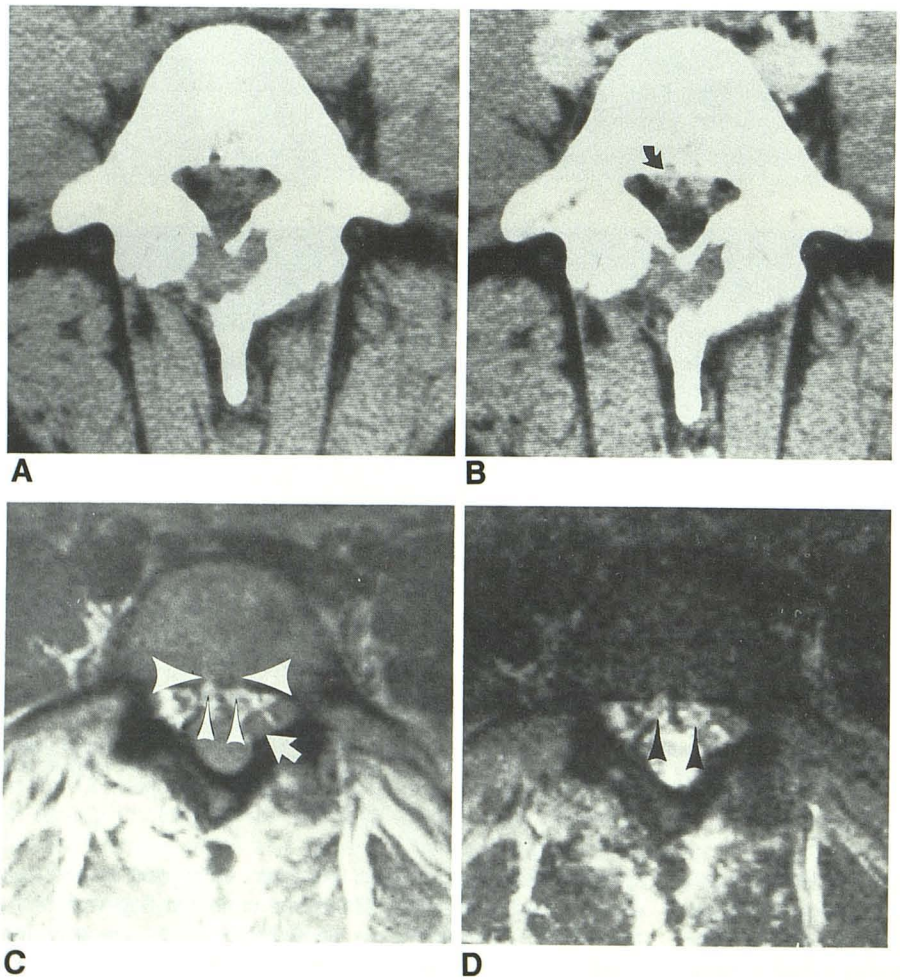

Fig. 7.—*A* and *B*, Pre- and post- IV CT scans at mid L5 level. Enhancement of basivertebral vein (*arrow*) and associated retrocorporeal anastomoses of veins.

C, Axial MR image (TR = 2000 msec, TE = 30 msec) at mid L5 level. *Arrow* indicates S1 component of conjoint L5–S1 nerve-root sleeves. Note hyperintense retrocorporeal anastomoses (*small arrowheads*) and basivertebral veins (*large arrowheads*).

D, Axial MR image (TR = 2000 msec, TE = 90 msec) at mid L5 level. Veins are again noted to be hyperintense (*arrowheads*).

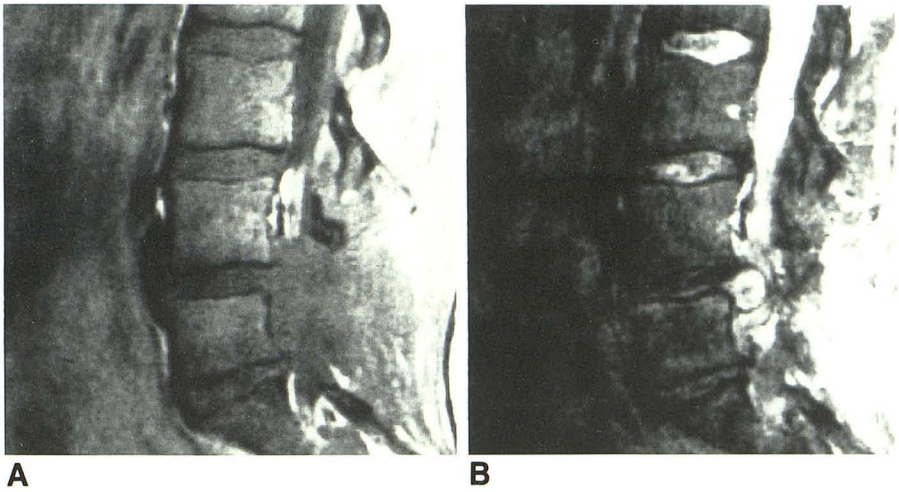

Fig. 8.—Case 14: free disk fragment and epidural scar.

***A*, Sagittal MR image (TR = 500 msec, TE = 17 msec) off midline to left. Large soft-tissue mass appears contiguous with posterior margin of L4–L5 disk occupying almost entire left lateral neural canal. Posterior margin of soft-tissue mass is indistinct as it merges with posterior paraspinal soft tissues.**

***B*, Sagittal MR image (TR = 2000 msec, TE = 90 msec) through same plane. Central portion of this region of soft tissue now shows well-circumscribed oval mass of increased signal intensity surgically proved to be free disk fragment. Note high signal intensity of scar tissue surrounding mass, both of which are similar to adjacent CSF. L4–L5 disk shows marked decrease in signal intensity consistent with severe degenerative changes.**

the multiple MR appearances of these vessels [21, 22]. The asymmetric, multiecho technique used in our study did not allow the phenomenon of even-echo rephasing to be appreciated.

Surface-coil MR has the advantage of demonstrating a larger area than IV CT does. It also has multidimensional imaging capabilities, providing orthogonal views for further characterization of a region. The disadvantages of MR include lack of conspicuity of cortical bone, poorer spatial resolution secondary to interslice gap, and, most importantly, decreased signal-to-noise on T2-weighted images. Parenthetically, this latter factor, coupled with technical difficulties, was responsible for the dropout of seven of the initially enrolled patients. Other minor disadvantages that have been reported previously include the cost; the potential for inducing claustrophobia; and the inability to image patients with aneurysm clips, pacemakers, and other types of metallic foreign bodies.

Prospective studies of IV CT with surgical confirmation of findings have shown an accuracy of 74–87% [5–7]. A similar accuracy was found in our small group. The procedure, however, is not without problems, and IV CT has been controversial in recent years.

Contrast enhancement on CT is related to the concentration of iodinated molecules within vascular lumina as well as their dispersion into the local extracellular spaces via intercellular gaps and the intracellular process pinocytosis [17, 19]. The ability to document vascular density along with the easy detectability of iatrogenic and degenerative bone changes are the strengths of IV CT. Its disadvantages include some operator dependence, radiation, the high iodine load (87.6 gI), and the ability to effectively examine only one disk space per session.

The reason for the uniform enhancement of scar on IV CT and the lack of enhancement of disk is said to be related to the local vascular density [6, 12]. The peripheral anulus has also been specifically reported not to enhance [14]. We have noted that a significant number of scars, particularly in a posterior epidural location, do not enhance (Fig. 5), whereas disk surfaces that are directly exposed to the surrounding paravertebral tissues occasionally do enhance. Anular and herniated disk enhancement has also been described recently [7, 23]. Thus, although an increase in local vascular density is presumed to be the means of scar enhancement on IV CT, the true mechanism is by no means totally clear.

In a sense, our study of the FBSS is incomplete. Neither MR nor IV CT findings were correlated with patient symptoms, nor were clinical follow-up findings included that would help determine the impact of these studies on the overall success rate of reoperation. In addition, a large patient population with surgical verification of findings would have been desirable, as would have been an attempt to assess the changes in scan appearances over time. Nevertheless, the results of this study suggest that MR may represent a noninvasive, initial test in the diagnostic evaluation of FBSS, with IV CT reserved for situations in which MR results are equivocal.

ACKNOWLEDGMENTS

We thank Lee Stein and Michele Williams for help in manuscript preparation.

REFERENCES

1. Burton CV, Kirkaldy-Willis WH, Yong-Hing K, Heithoff KB. Causes of failure of surgery on the lumbar spine. *Clin Orthop* **1981**;157:191–199
2. Burton CV. Lumbosacral arachnoiditis. *Spine* **1978**;3(1):24–30
3. Jorgensen J, Hansen PH, Steenskuv V, Oveson N. A clinical and radiological study of chronic lower arachnoiditis. *Neuroradiology* **1975**;9:133–144
4. Law JD, Lehman RAW, Kirsch WM. Reoperation after lumbar intervertebral disc surgery. *J Neurosurg* **1978**;48:259–263
5. Braun IF, Hoffman JC, David PC, Landman JA, Tindall GT. Contrast enhancement in CT differentiation between recurrent disc herniation and postoperative scar: prospective study. *AJNR* **1985**;6:607–617, *AJR* **1985**;145:785–790
6. Teplick JG, Haskin ME. Intravenous contrast-enhanced CT of the postoperative lumbar spine: improves identification of recurrent disc herniation, scar, arachnoiditis, and diskitis. *AJR* **1984**;143:845–855, AJNR **1984**; 5:373–383
7. Firooznia H, Kricheff II, Rafii M, Golimbu C. Lumbar spine after surgery: examination with intravenous contrast-enhanced CT. *Radiology* **1987**;163:221–226
8. Maravilla KR, Lesh P, Weinreb JC, Selby DK, Mooney V. Magnetic resonance imaging of the lumbar spine with CT correlation. *AJNR* **1985**;5: 237–245
9. Modic MT, Pavlicek W, Weinstein MA, et al. Magnetic resonance imaging

of intervertebral disc disease clinical and pulse sequence considerations. *Radiology* **1984**;152:103–111
10. Braun IF, Lin JP, Benjamin MV, Kricheff II. Computed tomography of the asymptomatic postsurgical lumbar spine: analysis of the physiologic scar. *AJNR* **1983**;4:1213–1216, *AJR* **1984**;142:149–152
11. Mall JC, Kaiser JA, Heithoff KB. Postoperative spine. In: Newton TH, Potts DG, eds. *Computed tomography of the spine and spinal cord*. San Anselmo, CA: Clavadel, **1983**:187–203
12. Schubiger O, Valavanis A. CT differentiation between recurrent disc herniation and postoperative scar formation: the value of contrast enhancement. *Neuroradiology* **1982**;22:251–254
13. Teplick JG, Haskin ME. CT of the postoperative lumbar spine. *Radiol Clin North Am* **1983**;21:395–420
14. Teplick JG, Haskin ME. Computed tomography of the postoperative lumbar spine. *AJNR* **1983**;4:1053–1073, *AJR* **1983**;141:865–884
15. Berne RM, Levy MN. *Cardiovascular physiology*, 2d ed. St. Louis: Mosby, **1972**:3
16. Edelman RR, Shoukimas GM, Stark DR, et al. High-resolution surface-coil imaging of lumbar disk disease. *AJNR* **1985**;6:479–485
17. Norman D, Steven EA, Wing SD, Levin V, Newton TH. Quantitative aspects of contrast enhancement in cranial computed tomography. *Radiology* **1978**;129:683–688
18. Bradley WG, Waluch V. Blood flow: magnetic resonance imaging. *Radiology* **1985**;154:443–450
19. Sage MR. Review. Blood brain barrier: phenomenon of increasing importance to the imaging clinician. *AJR* **1982**;138:887–898
20. Wehrli FW, MacFall JR, Shutts D, Breger R, Herfkens RJ. Mechanisms of contrast in NMR imaging. *J Comput Assist Tomogr* **1984**;8(3):369–380
21. Bradley WA, Waluch V, Lai K, Fernandez EJ, Spalter C. The appearance of rapidly flowing blood in magnetic resonance images. *AJR* **1984**;143:1167–1174
22. vonSchulthess GV, Higgins CB. Blood flow with MR: spin-phase phenomena. *Radiology* **1985**;157:687–695
23. Yang PJ, Seeger JF, Dzioba RB, Carmody RF, Burt TB. High-dose IV enhancement in CT scanning of the postoperative lumbar spine (abstr). *AJNR* **1985**;6:476